

Bayesian Integrals on Toric Varieties

Michael Borinsky, Anna-Laura Sattelberger,
Bernd Sturmfels, and Simon Telen

Abstract

We explore the positive geometry of statistical models in the setting of toric varieties. Our focus lies on models for discrete data that are parameterized in terms of Cox coordinates. We develop a geometric theory for computations in Bayesian statistics, such as evaluating marginal likelihood integrals and sampling from posterior distributions. These are based on a tropical sampling method for evaluating Feynman integrals in physics. We here extend that method from projective spaces to arbitrary toric varieties.

1 Introduction

Every projective toric variety X is a positive geometry [1]. Its canonical differential form Ω_X has poles on the toric boundary, and it encodes probability measures on the positive part $X_{>0}$. Our aim is to develop the geometry of Bayesian statistics in this toric setting. We introduce parametric statistical models by mapping $X_{>0}$ into a probability simplex Δ_m . The probabilities are written in Cox coordinates on X . We shall use the canonical measure on $X_{>0}$ for marginal likelihood integrals and for sampling from the posterior distribution.

We begin with an example for the product of three projective lines $X = \mathbb{P}^1 \times \mathbb{P}^1 \times \mathbb{P}^1$. This toric threefold has six Cox coordinates $x_0, x_1, s_0, s_1, t_0, t_1$. Each letter refers to homogeneous coordinates on one of the three lines \mathbb{P}^1 . We consider the model $X_{>0} \rightarrow \Delta_m$ parameterized by

$$p_\ell = \binom{m}{\ell} \frac{x_0}{x_0 + x_1} \frac{s_0^\ell s_1^{m-1}}{(s_0 + s_1)^m} + \binom{m}{\ell} \frac{x_1}{x_0 + x_1} \frac{t_0^\ell t_1^{m-\ell}}{(t_0 + t_1)^m} \quad \text{for } \ell = 0, 1, \dots, m. \quad (1)$$

These expressions are rational functions on X , positive on $X_{>0}$, and their sum equals 1. This is the conditional independence model for m binary random variables with binary hidden state. Algebraically, it represents symmetric $2 \times 2 \times \dots \times 2$ tensors of nonnegative rank 2.

For an intuitive understanding, imagine a gambler who has three biased coins, one in each hand, and one more to decide which hand to use. The latter coin has probabilities x_0 and x_1 for tails and heads, and this decides whether the left hand coin (with bias s_0, s_1) or the right hand coin (with bias t_0, t_1) is to be used. The gambler performs m coin tosses with the chosen hand and records the number of heads. The probability of observing ℓ heads equals p_ℓ . A more familiar formula for this event arises by dehomogenizing via $x_1 = x$, $x_0 = 1 - x$, etc:

$$p_\ell = \binom{m}{\ell} \left[(1-x)(1-s)^\ell s^{m-\ell} + x(1-t)^\ell t^{m-\ell} \right] \quad \text{for } \ell = 0, 1, \dots, m. \quad (2)$$

As is customary in toric geometry, we identify the positive variety $X_{>0}$ with the open cube $(0, 1)^3$, which is the space of dehomogenized parameters (x, s, t) . At first glance, the passage from (2) to (1) does not change much. It is a reparameterization of the model in $\Delta_m = \mathbb{P}_{>0}^m$, which comprises positive Hankel matrices that are semidefinite and have rank ≤ 2 . For instance, for $m = 4$ coin tosses, these are the 3×3 Hankel matrices shown in [8, Section 1]:

$$\begin{pmatrix} 12p_0 & 3p_1 & 2p_2 \\ 3p_1 & 2p_2 & 3p_3 \\ 2p_2 & 3p_3 & 12p_4 \end{pmatrix} = \frac{12}{x_0 + x_1} \begin{pmatrix} s_1^2 & t_1^2 \\ s_0s_1 & t_0t_1 \\ s_0^2 & t_0^2 \end{pmatrix} \begin{pmatrix} \frac{x_0}{(s_0 + s_1)^4} & 0 \\ 0 & \frac{x_1}{(t_0 + t_1)^4} \end{pmatrix} \begin{pmatrix} s_1^2 & s_0s_1 & s_0^2 \\ t_1^2 & t_0t_1 & t_0^2 \end{pmatrix}.$$

The key insight for what follows is that our toric 3-fold X has a canonical 3-form

$$\Omega_X = \sum_{i=0}^1 \sum_{j=0}^1 \sum_{k=0}^1 (-1)^{i+j+k} \frac{dx_i}{x_i} \wedge \frac{ds_j}{s_j} \wedge \frac{dt_k}{t_k}. \quad (3)$$

This gives $(X, X_{>0})$ the structure of a positive geometry in the sense of [1]. The associated representations of prior distributions on the parameter space $X_{>0}$ offers novel tools for Bayesian inference. For instance, suppose our prior belief about the parameters (x, s, t) in the coin model (2) is the uniform distribution on the cube $[0, 1]^3$. Its pullback to X equals

$$\Omega_X^{\text{unif}} = \frac{x_0x_1s_0s_1t_0t_1}{(x_0 + x_1)^2(s_0 + s_1)^2(t_0 + t_1)^2} \Omega_X. \quad (4)$$

Statistics is about data. If our gambler performs the experiment U times, and ℓ heads were observed u_ℓ times, then $\frac{1}{U}(u_0, u_1, \dots, u_m) \in \Delta_m$ is the empirical distribution. The likelihood function is a rational function on the toric variety X , namely $L_u = p_0^{u_0} p_1^{u_1} \cdots p_m^{u_m}$. The posterior distribution is the product of this function times the prior distribution on $X_{>0}$. For the prior that is uniform on $[0, 1]^3$ we take (4). The marginal likelihood integral equals

$$\int_{X_{>0}} p_0^{u_0} p_1^{u_1} \cdots p_m^{u_m} \Omega_X^{\text{unif}}. \quad (5)$$

Two important tasks in Bayesian statistics [7] are evaluating the integral (5) and sampling from the posterior distribution. See [10] and [15, Section 5.5] for points of entry from an algebraic perspective. In this paper we explore these tasks using toric and tropical geometry.

We shall study our statistical problem in the following algebraic framework. Let f and g be homogeneous polynomials of the same degree in the Cox coordinates on an n -dimensional toric variety X . We assume that all coefficients in f and g are positive real numbers, so the rational function f/g has no zeros or poles on $X_{>0}$. The integral of the n -form $(f/g)\Omega_X$ over the positive toric variety $X_{>0}$ is a positive real number, or it diverges. Our aim is to compute this number numerically. We focus on integrals of interest in Bayesian statistics.

The main contribution of this article is a geometric theory of Monte Carlo sampling, based on the positive geometry $(X, X_{>0})$. A central role is played by the canonical form Ω_X . The approach was first introduced in [2] for Feynman integrals on projective space $X = \mathbb{P}^n$.

Our presentation is organized as follows. Section 2 reviews the quotient construction of a toric variety X from its Cox ring. The canonical form Ω_X is defined in (10). We introduce integrals of the form $\int_{X_{>0}} (f/g)\Omega_X$, and we present a convergence criterion in Theorem 2.5.

In Section 3, we replace the rational function f/g in the integrand by its tropicalization. The resulting piecewise monomial structure divides the positive toric variety $X_{>0}$ into sectors. Theorem 3.8 gives a formula for integrating over each sector, against the tropical probability distribution on $X_{>0}$. Algorithm 3.12 offers a method for sampling from that distribution.

In Section 4, we develop a tropical approximation scheme for the classical integral $\int_{X_{>0}} (f/g)\Omega_X$. We apply rejection sampling to draw from the density induced by f/g on $X_{>0}$ with its canonical form Ω_X . The runtime is analyzed in terms of the acceptance rate.

Section 5 is devoted to discrete statistical models whose parameter space is a simple polytope P . Familiar instances are linear models, toric models, and their mixtures. We show how to pull back Bayesian priors from P to $X_{>0}$ via the moment map. The push-forward of Ω_X to P gives rise to the Wachspress model whose states are the vertices of P . The section concludes with a combinatorial analysis of the coin model in Equation (1).

In Section 6, we apply tropical integration and tropical sampling to data analysis in the Bayesian setting. We focus on the statistical models from Section 5, but now lifted from P to $X_{>0}$. We present algorithms, along with their implementation, for computing marginal likelihood integrals. Sampling from the posterior distribution is also discussed. Our software and other supplementary material for this article is available at the repository website [MathRepo](#) [5] of MPI-MiS via the link <https://mathrepo.mis.mpg.de/BayesianIntegrals>.

2 Toric Varieties and their Canonical Forms

We review the set-up of toric geometry, leading up to the integrals studied in this paper. For complete details we refer to the textbook [4] and the notes [17]. Let T be an n -dimensional complex algebraic torus with character lattice M and co-character lattice $N = \text{Hom}_{\mathbb{Z}}(M, \mathbb{Z})$. Fixing an isomorphism $T \simeq (\mathbb{C}^*)^n$ corresponds to identifying $M \simeq \mathbb{Z}^n$ and $N \simeq \mathbb{Z}^n$. We write χ^a for the character in M corresponding to the lattice point $a \in \mathbb{Z}^n$ and λ^v for the co-character in N corresponding to $v \in \mathbb{Z}^n$. The pairing $\langle \cdot, \cdot \rangle : N \times M \rightarrow \mathbb{Z}$ is given by $\langle \lambda^v, \chi^a \rangle = \chi^a \circ \lambda^v \in \text{Hom}_{\mathbb{Z}}(\mathbb{C}^*, \mathbb{C}^*) \simeq \mathbb{Z}$. In coordinates, this is the dot product $\langle v, a \rangle = v \cdot a$.

Fix a complete fan Σ in $\mathbb{R}^n = N \otimes_{\mathbb{Z}} \mathbb{R}$. The n -dimensional toric variety $X = X_{\Sigma} \supset T$ is normal and complete. Write $\Sigma(d)$ for the set of cones of dimension d in Σ , and $k = |\Sigma(1)|$ for the number of rays of Σ . Each ray $\rho \in \Sigma(1)$ has a primitive ray generator $v_{\rho} \in \mathbb{Z}^n$, satisfying $\rho \cap \mathbb{Z}^n = \mathbb{N} \cdot v_{\rho}$. We collect the rays in the columns of the $n \times k$ matrix $V = [v_1 \ v_2 \ \cdots \ v_k]$.

The free group of torus-invariant Weil divisors on X is $\text{Div}_T(X) = \bigoplus_{\rho} \mathbb{Z} \cdot D_{\rho} \simeq \mathbb{Z}^k$. A character $\chi^a \in M$ extends to a rational function on X with divisor $\text{div}(\chi^a) = \sum_{\rho} \langle v_{\rho}, a \rangle D_{\rho}$. The transpose matrix V^{\top} , viewed as a map of lattices $M \rightarrow \text{Div}_T(X) \simeq \mathbb{Z}^k$, sends a character to its divisor. Two torus-invariant divisors $D_1, D_2 \in \text{Div}_T(X)$ are linearly equivalent if and only if $D_1 - D_2 = \text{div}(\chi^a)$ for some character χ^a . Equivalently, there is an exact sequence

$$0 \longrightarrow M \xrightarrow{V^{\top}} \mathbb{Z}^k \longrightarrow \text{Cl}(X) \longrightarrow 0. \quad (6)$$

The cokernel $\text{Cl}(X) = \mathbb{Z}^k / \text{im} V^{\top}$ is the *divisor class group* of X . The *Picard group* $\text{Pic}(X) \subseteq \text{Cl}(X)$ is the subgroup of Cartier divisors modulo linear equivalence. Applying the functor $\text{Hom}_{\mathbb{Z}}(-, \mathbb{C}^*)$ to (6), we obtain the following exact sequence of multiplicative abelian groups:

$$1 \longrightarrow G \longrightarrow (\mathbb{C}^*)^k \longrightarrow (\mathbb{C}^*)^n \longrightarrow 1. \quad (7)$$

The group $G = \text{Hom}_{\mathbb{Z}}(\text{Cl}(X), \mathbb{C}^*)$ is reductive: it is a quasi-torus of dimension $k - n$.

We now introduce the polynomial ring $S = \mathbb{C}[x_1, \dots, x_k]$, with one variable x_ρ for each divisor D_ρ , $\rho \in \Sigma(1)$. The sequence (6) defines a grading of S by the group $\text{Cl}(X)$, and the sequence (7) gives the associated quasi-torus action by G on the affine space $\text{Spec}(S) = \mathbb{C}^k$.

The toric variety X can be realized as a quotient $(\mathbb{C}^k \setminus \mathcal{V}(B)) // G$. The *irrelevant ideal* $B \triangleleft S$ is generated by the squarefree monomials $x^\sigma = \prod_{\rho \notin \sigma} x_\rho$ representing maximal cones, i.e.,

$$B = \langle x^\sigma \mid \sigma \in \Sigma(n) \rangle.$$

The map $(\mathbb{C}^*)^k \rightarrow (\mathbb{C}^*)^n$ in (7) is constant on G -orbits. It is the restriction of the map $\pi : \mathbb{C}^k \setminus \mathcal{V}(B) \rightarrow X$ which presents X as the quotient above. The notation $//$ indicates that this is generally not a *geometric* quotient. However, it is if Σ is a simplicial fan. Under this extra assumption, we write $X = (\mathbb{C}^k \setminus \mathcal{V}(B)) / G$ and there is a one-to-one correspondence

$$\{G\text{-orbits in } \mathbb{C}^k \setminus \mathcal{V}(B)\} \xleftrightarrow{1:1} \{\text{points in } X\}.$$

The polynomial ring S is the *Cox ring* of X . It is graded by the group $\text{Cl}(X) = \mathbb{Z}^k / \text{im} V^\top$,

$$S = \bigoplus_{\gamma \in \text{Cl}(X)} S_\gamma, \quad \text{where} \quad S_\gamma = \bigoplus_{a: V^\top a + c \geq 0} \mathbb{C} \cdot x^{V^\top a + c}.$$

The vector $c \in \mathbb{Z}^k$ is fixed. It represents any divisor $D_c = \sum_\rho c_\rho D_\rho$ such that $[D_c] = \gamma$. The sum on the right is over all $a \in M$ such that the integer vector $V^\top a + c$ is nonnegative.

The zero locus in \mathbb{C}^k of a homogeneous polynomial $f \in S$ is stable under the G -action. Hence the zero locus of f in X is well-defined. In fact, homogeneous ideals of S define subschemes of X , and all subschemes arise in this way. If X is smooth, then the subschemes of X are in one-to-one correspondence with the B -saturated homogeneous ideals of S .

The material above may look overly formal to a novice. Yet, toric varieties X and their Cox coordinates x_1, \dots, x_k are practical tools for applications, e.g., in the numerical solution of polynomial equations [16]. The present paper extends the utility of the abstract setting to numerical computing at the interface of statistics and physics [2, 14]. In applications, the toric variety X is usually projective, i.e., Σ is the normal fan of a lattice polytope in \mathbb{R}^n .

Example 2.1 (3-cube). Let $n = 3$, $k = 6$ and Σ the fan given by the eight orthants in \mathbb{R}^3 . Then $X = \mathbb{P}^1 \times \mathbb{P}^1 \times \mathbb{P}^1$, with Cox ring $S = \mathbb{C}[x_0, x_1, s_0, s_1, t_0, t_1]$, graded by $\text{Cl}(X) = \mathbb{Z}^3$. The irrelevant ideal is $B = \langle x_0, x_1 \rangle \cap \langle s_0, s_1 \rangle \cap \langle t_0, t_1 \rangle = \langle x_0 s_0 t_0, x_0 s_0 t_1, \dots, x_1 s_1 t_1 \rangle$. We represent X as the quotient of $\mathbb{C}^6 \setminus \mathcal{V}(B)$ modulo the action $G = (\mathbb{C}^*)^3$, as in the Introduction. See [11, Example 6.2.7 (2)] for a detailed study of this example and its tropicalization. \diamond

Example 2.2 (Pentagon). Let $n = 2$, $k = 5$ and Σ the normal fan of the polygon in Figure 1. The rays of Σ are the inner normals to the edges. We write their generators in the matrix

$$V = \begin{pmatrix} 1 & 1 & -1 & -1 & 0 \\ 0 & -1 & -1 & 1 & 1 \end{pmatrix}. \quad (8)$$

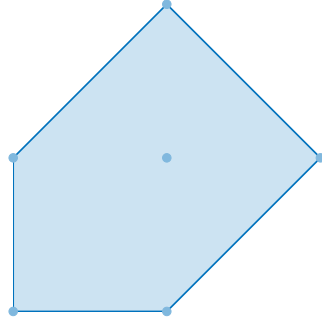


Figure 1: This pentagon specifies the projective toric surface in Example 2.2.

We have $G \simeq (\mathbb{C}^*)^3$, since $\text{Cl}(X) = \mathbb{Z}^5/\text{im } V^\top$ is isomorphic to \mathbb{Z}^3 . The irrelevant ideal is

$$B = \langle x_1x_2x_3, x_2x_3x_4, x_3x_4x_5, x_4x_5x_1, x_5x_1x_2 \rangle \triangleleft S = \mathbb{C}[x_1, x_2, x_3, x_4, x_5].$$

The quotient map $(x_1, \dots, x_5) \mapsto (x_1x_2x_3^{-1}x_4^{-1}, x_2^{-1}x_3^{-1}x_4x_5)$ represents X as $(\mathbb{C}^5 \setminus \mathcal{V}(B))/G$.

We find it convenient to write the image of V^\top in \mathbb{Z}^5 as the kernel of another matrix, e.g.,

$$W = \begin{pmatrix} 0 & 1 & 0 & 1 & 0 \\ 1 & 0 & 1 & 0 & 1 \\ 2 & 0 & 1 & 1 & 0 \end{pmatrix}. \quad (9)$$

The \mathbb{Z}^3 -grading of S is given by sending x_i to the i -th column of W . The G -action on \mathbb{C}^5 is

$$x_1 \mapsto t_2t_3^2x_1, \quad x_2 \mapsto t_1x_2, \quad x_3 \mapsto t_2t_3x_3, \quad x_4 \mapsto t_1t_3x_4, \quad x_5 \mapsto t_2x_5.$$

If $c \in \mathbb{Z}^5$, then $\gamma = Wc \in \mathbb{Z}^3$ represents the class $[D_c] \in \text{Cl}(X)$ of the divisor D_c on X . \diamond

The positive orthant $\mathbb{R}_{>0}^k$ is disjoint from $\mathcal{V}(B)$ since B is a monomial ideal. We can restrict the quotient map $\mathbb{R}^k \setminus \mathcal{V}(B) \rightarrow X$ to $\mathbb{R}_{>0}^k$. The image of this restriction is the *positive part* $X_{>0}$ of the toric variety X . The Euclidean closure of $X_{>0}$ in X is denoted $X_{\geq 0}$. If X is projective with polytope P then the moment map gives a homeomorphism from $X_{>0}$ onto P° .

Motivated by statistics (see Equation (5)), we wish to integrate *meromorphic* n -forms with poles outside $X_{>0}$ over the nonnegative part $X_{\geq 0}$. We here describe an explicit representation of such forms via the Cox ring S . For any n -element subset $I \subset \Sigma(1)$, let $\det(V_I)$ denote the minor of V indexed by I . We define a meromorphic n -form on \mathbb{C}^k as follows:

$$\Omega_X = \sum_{\substack{I \subset \Sigma(1), \\ |I|=n}} \det(V_I) \bigwedge_{\rho \in I} \frac{dx_\rho}{x_\rho}. \quad (10)$$

This is the *canonical form* of the pair $(X, X_{\geq 0})$, viewed as a *positive geometry*, as explained by Arkani-Hamed, Bai, and Lam in [1, Section 5.6.2]. The canonical form Ω_X is the pullback under the quotient map π of the T -invariant n -form $\bigwedge_{j=1}^n \frac{dt_j}{t_j} \in \Omega_T^n(T)$, where $t_j = \chi^{e_j}$ are coordinates on T . This follows from [4, Cor. 8.2.8] by observing that $\pi^*(t_j) = \prod_{i=1}^k x_\rho^{\langle v_i, e_j \rangle}$.

After scaling by a rational function, the canonical form Ω_X defines a probability measure on $X_{>0}$. We are interested in the definite integral of the form $(f/g)\Omega_X$ over that space:

$$\mathcal{I} = \int_{X_{>0}} \frac{f}{g} \Omega_X. \quad (11)$$

The integrals \mathcal{I} appear as Feynman integrals in physics. The article [2] introduces tropical sampling for Feynman integrals over the projective space $X = \mathbb{P}^n$. The present paper generalizes that approach to the setting where X can be any toric variety.

Remark 2.3. The canonical form Ω_X of a toric variety X is closely related to the canonical sheaf ω_X . Indeed, by the discussion following [4, Corollary 8.2.8], ω_X is the sheaf of the cyclic graded S -module generated by the n -form $(\prod_{i=1}^k x_i) \Omega_X$. See also [3, Proposition 2.1]. \diamond

We next explain how to understand and evaluate the integral (11). Let $\gamma = \deg(f) = \deg(g) \in \text{Cl}(X)$ denote the class of the divisor D_c . The canonical isomorphism

$$S_\gamma = \bigoplus_{a: V^\top a + c \geq 0} \mathbb{C} \cdot x^{V^\top a + c} \simeq \bigoplus_{a: V^\top a + c \geq 0} \mathbb{C} \cdot t^a$$

represents *dehomogenization*. It sends f and g to Laurent polynomials \hat{f} and \hat{g} respectively.

This is compatible with the quotient map $\pi : \mathbb{C}^k \setminus \mathcal{V}(B) \rightarrow X$ in the following way. The map of tori $\pi_{|(\mathbb{C}^*)^k} : (\mathbb{C}^*)^k \rightarrow T \subset X$ realizes the torus of X as a geometric quotient $T \simeq (\mathbb{C}^*)^k / G$. Further restricting to the positive part gives $T_{>0} \simeq X_{>0}$. Let $\phi : X_{>0} \rightarrow T_{>0}$ denote this diffeomorphism. In Cox coordinates, ϕ is the monomial map given by the rows of V , see Example 2.2. One checks easily that the functions $(f/g) : X_{>0} \rightarrow \mathbb{C}$ and $(\hat{f}/\hat{g}) : T_{>0} \rightarrow \mathbb{C}$ satisfy $(f/g) = (\hat{f}/\hat{g}) \circ \phi$. Moreover, Ω_X restricted to its dense torus is the form $\pi^* \left(\bigwedge_{j=1}^n \frac{dt_j}{t_j} \right)$ which, in turn, uniquely determines Ω_X . Those observations imply

Proposition 2.4. *The integral (11) equals a more familiar integral over $T_{>0} = \mathbb{R}_{>0}^n$, namely*

$$\mathcal{I} = \int_{T_{>0}} \frac{\hat{f}}{\hat{g}} \bigwedge_{j=1}^n \frac{dt_j}{t_j}. \quad (12)$$

We conclude the section with a result on convergence. This generalizes [2, Theorem 3].

Theorem 2.5. *Suppose that the Newton polytope of the denominator g is n -dimensional and contains that of the numerator f in its relative interior. Then the integral (11) converges.*

Proof. We use the formulation in (12). By linearity of the integral, it suffices to consider the case when f is a monomial. In that special case, our integral can be viewed as the Mellin transform of the polynomial g . Therefore, the analysis given by Nilsson and Passare in [12] can be applied here. Their result is stated for integrals over $T_{\geq 0} = \mathbb{R}_{\geq 0}^n$, so we can use it for (12). The convergence result then follows from [12, Theorem 1]. \square

Remark 2.6. The hypothesis of Theorem 2.5 will be satisfied for the Bayesian integrals that arise from our statistical models in Sections 5 and 6. For instance, consider the integrand in (4). The Newton polytope of the denominator is the standard 3-cube scaled by a factor of two. Its unique lattice point is the Newton polytope of the monomial in the numerator. \diamond

3 Tropical Sampling

Our aim is to evaluate the integral \mathcal{I} in (11) and (12). To this end, it is convenient to consider a tropicalized version of the integral. Following [2], we define the *tropical approximation* of a polynomial $f \in S = \mathbb{C}[x_1, \dots, x_k]$ to be the following piecewise monomial function:

$$f^{\text{tr}}: \mathbb{R}_{>0}^k \longrightarrow \mathbb{R}_{>0}, \quad x \mapsto \max_{\ell \in \text{supp}(f)} x^\ell.$$

This definition differs in two aspects from the textbook definition of tropicalization in [11]. First, we adopt the max-convention. Second, we use the monomials x^ℓ instead of the linear forms $\langle x, \ell \rangle$. Thus f^{tr} is the exponential of the piecewise-linear convex function $\text{trop}(f)$.

If $f \in S \setminus \{0\}$ is homogeneous with positive coefficients, then the ratio $f(x)/f^{\text{tr}}(x)$ is a well-defined function on $\mathbb{R}_{>0}^k \subset \mathbb{C}^k \setminus \mathcal{V}(B)$ and is constant on G -orbits. It induces a function $X_{>0} \rightarrow \mathbb{R}_{>0}$, which takes $x \in X_{>0}$ to $f(x')/f^{\text{tr}}(x')$ for any $x' \in \pi^{-1}(x)$. Employing a slight abuse of notation, the expression $f(x)/f^{\text{tr}}(x)$ also denotes that function on $X_{>0}$.

As a special case of [2, Theorems 8A and 8B], where also polynomials with negative or complex coefficients are allowed, such functions are bounded above and below as follows.

Proposition 3.1. *Suppose that the homogeneous polynomial $f(x) = \sum_{\ell \in \text{supp}(f)} f_\ell x^\ell$ has positive coefficients, and set $C_1 = \min_{\ell \in \text{supp}(f)} f_\ell$ and $C_2 = \sum_{\ell \in \text{supp}(f)} f_\ell$. Then, we have*

$$0 < C_1 \leq \frac{f(x)}{f^{\text{tr}}(x)} \leq C_2 < \infty \quad \text{for all } x \in X_{>0}.$$

We assume from now on that f and g are homogeneous polynomials in S , with positive coefficients, of the same degree in $\text{Cl}(X)$, and that the hypothesis of Theorem 2.5 is satisfied.

Corollary 3.2. *The following integral over the positive toric variety $X_{>0}$ is finite:*

$$\mathcal{I}^{\text{tr}} = \int_{X_{>0}} \frac{f^{\text{tr}}}{g^{\text{tr}}} \Omega_X. \quad (13)$$

Proof. The tropical rational function $f^{\text{tr}}/g^{\text{tr}}$ is positive on $X_{>0}$ and it is bounded above by a constant times the classical function f/g . This follows by applying Proposition 3.1 to both f and g . Since the integral over f/g is finite, so is the integral over $f^{\text{tr}}/g^{\text{tr}}$. \square

The function $f^{\text{tr}}/g^{\text{tr}}$ is piecewise monomial on $X_{>0}$. The pieces are certain sectors, to be described below. The integral of each monomial over its sector is given in Theorem 3.8. The value of \mathcal{I}^{tr} is the sum (18) of the sector integrals. Here is an illustration for the integral \mathcal{I}^{tr} .

Example 3.3 (Classical integral versus tropical integral). We fix the projective line $X = \mathbb{P}^1$ with coordinates $(x_0 : x_1)$. The following binary cubics satisfy our convergence hypotheses:

$$f = x_0^2 x_1 \quad \text{and} \quad g = (x_0 + x_1)(x_0 + 3x_1)(5x_0 + x_1).$$

The corresponding tropical polynomial functions on the line segment $X_{\geq 0} = \mathbb{P}_{\geq 0}^1$ are

$$f^{\text{tr}} = f = x_0^2 x_1 \quad \text{and} \quad g^{\text{tr}} = \begin{cases} x_0^3 & \text{if } x_0 \geq x_1, \\ x_1^3 & \text{if } x_0 \leq x_1. \end{cases}$$

The classical integral (11) evaluates to $\frac{1}{56}(6 \ln(3) - \ln(5)) = 0.088968\dots$. We find this on either chart $\{x_0 = 1\}$ or $\{x_1 = 1\}$. The tropical integral (13) evaluates to $1 + \frac{1}{2} = \frac{3}{2}$. Here we integrate the two monomials in $f^{\text{tr}}/g^{\text{tr}}$ over the sectors $\{x_0 \geq x_1\}$ and $\{x_0 \leq x_1\}$. \diamond

Based on the idea that the tropical integral is easier to compute, we now rewrite (11) as

$$\mathcal{I} = \int_{X_{>0}} \frac{f}{g} \Omega_X = \mathcal{I}^{\text{tr}} \cdot \int_{X_{>0}} h \mu_{f,g}^{\text{tr}}, \quad (14)$$

where

$$h = \frac{f \cdot g^{\text{tr}}}{g \cdot f^{\text{tr}}} \quad \text{and} \quad \mu_{f,g}^{\text{tr}} = \frac{1}{\mathcal{I}^{\text{tr}}} \frac{f^{\text{tr}}}{g^{\text{tr}}} \Omega_X.$$

The function h is positive and bounded on $X_{>0}$, again by Proposition 3.1. The differential form $\mu_{f,g}^{\text{tr}}$ is nonnegative on $X_{>0}$, and it integrates to 1. In symbols, $\int_{X_{>0}} \mu_{f,g}^{\text{tr}} = 1$.

From a statistical perspective, the following function is a *probability density* on $X_{>0}$:

$$d_{f,g}^{\text{tr}} := \frac{1}{\mathcal{I}^{\text{tr}}} \frac{f^{\text{tr}}}{g^{\text{tr}}}. \quad (15)$$

We refer to it as the *tropical density*. In those terms, $\mu_{f,g}^{\text{tr}} = d_{f,g}^{\text{tr}} \cdot \Omega_X$ is a *probability measure* on $X_{>0}$ and the pair $(X_{>0}, \mu_{f,g}^{\text{tr}})$ is a *probability space*. For basic terminology from probability, we refer to the textbook [13], and to the guided tours in [7, Chapter 1] and [15, Chapter 2].

If we are able to draw samples from the distribution defined by the tropical density, then we can use *Monte Carlo integration* to estimate the integral (11). Furthermore, using *rejection sampling*, we can also produce samples from the classical density $d_{f,g} = \frac{1}{\mathcal{I}} \frac{f}{g}$ on $X_{>0}$, where the value of the integral (11) plays the role of a normalization factor. We will describe these computations in the next section. They play a fundamental role in Bayesian inference. For an introduction to Bayesian statistics see [7].

In the remainder of this section, we present our *tropical sampling algorithm*, for sampling from the probability distribution on $X_{>0}$ that is given by the tropical density $d_{f,g}^{\text{tr}}$. This algorithm was introduced in [2] for the special case of projective space $X = \mathbb{P}^n$, and it was successfully applied to Feynman integrals. We here extend it to other toric varieties X .

The Newton polytopes $\mathcal{N}(f)$ and $\mathcal{N}(g)$ of the homogeneous polynomials f and g live in \mathbb{R}^k , but their dimension is at most n , since they lie in an affine translate of $\text{im}_{\mathbb{R}}(V^{\top}) \simeq \mathbb{R}^n$. In light of Theorem 2.5, $\mathcal{N}(g)$ has the maximal dimension n . We are interested in the normal fan of the n -dimensional polytope $\mathcal{N}(f) + \mathcal{N}(g) = \mathcal{N}(fg)$, which lies in a different affine translate of $\text{im}_{\mathbb{R}}(V^{\top})$. Its normal fan has the lineality space $K := \ker(V) \simeq \mathbb{R}^{k-n}$, so that fan can be seen as a pointed fan in $\mathbb{R}^k/K \simeq \mathbb{R}^n$. We fix a simplicial refinement \mathcal{F} of this normal fan. Each maximal cone of \mathcal{F} is spanned by n linearly independent vectors, and the union of these cones covers \mathbb{R}^k/K . We alert the reader that there are now two different fans: Σ is the fan of the toric variety X , whereas \mathcal{F} comes from our polynomials f and g .

Example 3.4. In the application to Feynman integrals in [2], the polynomials f and g are *Symanzik polynomials*. Their Newton polytopes are *generalized permutohedra* [2, Section 6]. For such integrals, we can take \mathcal{F} to be the fan determined by the hyperplanes $\{x_i = x_j\}$. The computational results in [2, Section 7.4] rely on this special combinatorial structure. \diamond

We now abbreviate $e^y = (e^{y_1}, \dots, e^{y_k})$, and we define the *exponential map*

$$\text{Exp} : \mathbb{R}^k / K \rightarrow X_{>0}, \quad [(y_1, \dots, y_k)] \mapsto \pi(e^y). \quad (16)$$

This map is well-defined because the subspace K is mapped into the image of G under the abelian group homomorphism $\mathbb{R}^k \rightarrow (\mathbb{C}^*)^k$, $y \mapsto e^y$, cf. the exact sequences (6) and (7).

Remark 3.5. The exponential map is an inverse to *tropicalization*. The coordinate-wise logarithm map $\mathbb{R}_{>0}^k \rightarrow \mathbb{R}^k$ turns the multiplicative action of G into an additive action of K . That is, it induces a map $\text{Log} : X_{>0} \rightarrow \mathbb{R}^k / K$. We refer to [11, Chapter 6] for details. \diamond

We continue to retain the hypotheses $\dim(\mathcal{N}(g)) = n$ and $\mathcal{N}(f) \subseteq \text{relint } \mathcal{N}(g)$.

Lemma 3.6. *For all nonzero elements $y \in \mathbb{R}^k / K$, we have*

$$\max_{\nu \in \mathcal{N}(g)} y \cdot \nu - \max_{\nu \in \mathcal{N}(f)} y \cdot \nu > 0. \quad (17)$$

Proof. The left hand side of the inequality is well-defined modulo K , because both Newton polytopes lie in the same affine translate of K . Suppose the two maxima are attained for $\nu_f \in \mathcal{N}(f)$ and $\nu_g \in \mathcal{N}(g)$. If $y \cdot \nu_g \leq y \cdot \nu_f$ were to hold, then ν_f lies in both $\mathcal{N}(f)$ and the boundary of $\mathcal{N}(g)$. This contradicts our hypothesis. We therefore have $y \cdot \nu_g > y \cdot \nu_f$. \square

Lemma 3.7. *Fix a cone σ in the simplicial fan \mathcal{F} and consider any vertices ν_f and ν_g of the corresponding faces of the Newton polytopes $\mathcal{N}(f)$ and $\mathcal{N}(g)$. Then*

$$\frac{f^{\text{tr}}(x)}{g^{\text{tr}}(x)} = x^{-(\nu_g - \nu_f)} \quad \text{for all } x \in \mathbb{R}^k \text{ such that } \pi(x) \in \text{Exp}(\sigma).$$

Proof. By definition of the normal fan, the two functions $y \mapsto \max_{\nu \in \mathcal{N}(f)} y \cdot \nu$ and $y \mapsto \max_{\nu \in \mathcal{N}(g)} y \cdot \nu$ are linear on the cone σ . Let $y \in \sigma$ satisfy $\text{Exp}(y) = x$. Then we have

$$\log f^{\text{tr}}(x) = \log \max_{\ell \in \text{supp}(f)} x^\ell = \max_{\ell \in \text{supp}(f)} \ell \cdot y = \max_{\nu \in \mathcal{N}(f)} \nu \cdot y = \nu_f \cdot y.$$

Similarly, $\log g^{\text{tr}}(x) = \nu_g \cdot y$. Applying the exponential function yields the assertion. \square

In order to evaluate the integral (11), we use the factorization in (14). The first task is to evaluate the tropical integral \mathcal{I}^{tr} . Since Exp is a bijection, we can use the decomposition

$$\mathcal{I}^{\text{tr}} = \sum_{\sigma \in \mathcal{F}(n)} \mathcal{I}_{\sigma}^{\text{tr}} \quad \text{where} \quad \mathcal{I}_{\sigma}^{\text{tr}} = \int_{\text{Exp}(\sigma)} \frac{f^{\text{tr}}}{g^{\text{tr}}} \Omega_X. \quad (18)$$

The positive toric variety $X_{>0}$ is partitioned into the *sectors* $\text{Exp}(\sigma)$. Each tropical integral $\mathcal{I}_{\sigma}^{\text{tr}}$ is the integral of a Laurent monomial of degree zero, namely $x^{-\delta_{\sigma}}$, where $\delta_{\sigma} = \nu_g - \nu_f$. The integral of $x^{-\delta_{\sigma}}$ over all of $X_{>0}$ diverges, but our combinatorial set-up ensures that it converges when restricted to the sector $\text{Exp}(\sigma)$. We saw this for $X = \mathbb{P}^1$ in Example 3.3.

We next present a formula for the integral $\mathcal{I}_{\sigma}^{\text{tr}}$. We fix a matrix $W = [w_1 \cdots w_n] \in \mathbb{R}^{k \times n}$ whose n column vectors w_{ℓ} generate the simplicial cone σ in \mathbb{R}^k / K .

Theorem 3.8. *The tropical sector integral in (18) is equal to*

$$\mathcal{I}_\sigma^{\text{tr}} = \frac{\det(VW)}{\prod_{\ell=1}^n w_\ell \cdot \delta_\sigma}. \quad (19)$$

Before proving (19), we offer a few remarks on its interpretation. The columns w_ℓ of W are only defined up to the equivalence in \mathbb{R}^k/K . Still, the numerator is well-defined, because $\det(VW) = \det(VW')$ for any choices of representatives in the matrix $W' = [w'_1 \cdots w'_n]$ with $w'_i = w_i + \lambda_i$ and $\lambda_i \in K = \ker V$. As $x^{-\delta_\sigma}$ has degree 0, we have $\delta_\sigma = \nu_g - \nu_f \in \text{im}_{\mathbb{R}}(V^\top) = K^\perp$. Thus, the denominator does not depend on the choice of representative for w_ℓ . Similarly, the lengths of the generators w_ℓ are irrelevant for the description of the cone. The quotient in (19) is invariant under rescalings of a vector $w_\ell \rightarrow \xi w_\ell$, as the multiplier ξ , which factors out of the determinant, cancels between the numerator and the denominator. The sign of the numerator depends on the ordering of the vectors w_ℓ in W which is arbitrary a priori. We arrange them in the matrix W so that the condition $\det(VW) > 0$ holds. Hence, the value of $\mathcal{I}_\sigma^{\text{tr}}$ is an invariant of the cone σ equipped with a positive orientation and the data V and δ_σ . By Lemma 3.6, we have $w_\ell \cdot \delta_\sigma > 0$ for all ℓ and hence $0 < \mathcal{I}_\sigma^{\text{tr}} < \infty$ for all σ .

Proof. From Lemma 3.7 and our discussion above, we know that

$$\mathcal{I}_\sigma^{\text{tr}} = \int_{\text{Exp}(\sigma)} x^{-\delta_\sigma} \Omega_X.$$

We expand Ω_X as in (10), and we change coordinates under the exponential map. This gives

$$\mathcal{I}_\sigma^{\text{tr}} = \int_{\sigma} e^{-y \cdot \delta_\sigma} \sum_{\substack{I \subset \Sigma(1), \\ |I|=n}} \det(V_I) \bigwedge_{i \in I} dy_i = \sum_{\substack{I \subset \Sigma(1), \\ |I|=n}} \det(V_I) \int_{\sigma} e^{-y \cdot \delta_\sigma} \bigwedge_{i \in I} dy_i. \quad (20)$$

On the right, we see the integral of the exponential of a linear form over a simplicial cone. Since σ is the image of $\mathbb{R}_{>0}^n$ under the linear map given by the $n \times n$ matrix W_I , we obtain

$$\int_{\sigma} e^{-y \cdot \delta_\sigma} \bigwedge_{i \in I} dy_i = \frac{\det(W_I)}{\prod_{\ell=1}^n w_\ell \cdot \delta_\sigma}.$$

The Cauchy–Binet formula $\det(VW) = \sum_I \det(V_I) \det(W_I)$ concludes the proof of (19). \square

The following result is a generalization of [2, Lemma 17]. For an arbitrary kernel ψ , the sector integral is transformed to the standard cube. Our proof technique is adapted from [2].

Proposition 3.9. *For any bounded function $\psi : X_{>0} \rightarrow \mathbb{R}$, we have*

$$\int_{\text{Exp}(\sigma)} \frac{f^{\text{tr}}}{g^{\text{tr}}} \psi \Omega_X = \mathcal{I}_\sigma^{\text{tr}} \cdot \int_{[0,1]^n} \psi(x^\sigma(q)) dq_1 \wedge \cdots \wedge dq_n, \quad (21)$$

where

$$x_i^\sigma(q) = \prod_{\ell=1}^n q_\ell^{-(w_\ell)_i/(w_\ell \cdot \delta_\sigma)} \quad \text{for } i = 1, 2, \dots, k. \quad (22)$$

In particular, the integral in (21) is finite for any cone $\sigma \in \mathcal{F}(n)$.

Proof. With the exponential map as in (20), the integral on the left can be written as

$$\sum_{\substack{I \subset \Sigma(1), \\ |I|=n}} \det(V_I) \cdot \int_{\sigma} e^{-y \cdot \delta_{\sigma}} \psi(\text{Exp}(y)) \bigwedge_{\rho \in I} dy_{\rho}. \quad (23)$$

Using coordinates λ on $\mathbb{R}_{>0}^n$, and writing $y_i = \sum_{\ell=1}^n \lambda_{\ell} (w_{\ell})_i$ for $i \in I$, the integral in (23) is

$$\det(W_I) \cdot \int_{\mathbb{R}_{>0}^n} e^{-(W\lambda) \cdot \delta_{\sigma}} \psi(\text{Exp}(W\lambda)) \prod_{\ell=1}^n d\lambda_{\ell}.$$

We finally transform the integral from $\mathbb{R}_{>0}^n$ to the cube $[0, 1]^n$ using the logarithm function. More precisely, we apply the transformation $\lambda_{\ell} = (w_{\ell} \cdot \delta_{\sigma})^{-1} \log(q_{\ell})$ for $\ell = 1, \dots, n$. This yields the right hand side in (21). This last step uses the fact that $w_{\ell} \cdot \delta_{\sigma} > 0$, which we know from Lemma 3.6. This fact, together with boundedness of ψ , implies convergence. \square

Remark 3.10. The formula (22) gives parameterizations of each sector by a standard cube:

$$x^{\sigma} : [0, 1]^n \rightarrow \text{Exp}(\sigma), \quad q \mapsto x^{\sigma}(q).$$

To digest the exponent in (22), note that the (i, ℓ) -th entry of W is the i th entry $(w_{\ell})_i$ of the vector w_{ℓ} , that δ_{σ} lies in K , and that the row vector $\delta_{\sigma} \cdot W$ has coordinates $w_{\ell} \cdot \delta_{\sigma}$. \diamond

We use the sector decomposition of $X_{>0}$ given by the fan \mathcal{F} to evaluate the integral (11). Rewriting (11) as in (14) and using the parameterizations $\text{Exp} : \mathbb{R}^k/K \rightarrow X_{>0}$ gives

$$\int_{X_{>0}} \frac{f}{g} \Omega_X = \int_{X_{>0}} \frac{f^{\text{tr}}}{g^{\text{tr}}} h \Omega_X = \sum_{\sigma \in \mathcal{F}(n)} \int_{\text{Exp}(\sigma)} \frac{f^{\text{tr}}}{g^{\text{tr}}} h \Omega_X. \quad (24)$$

Each integral on the right hand side is an integral over the cube by Proposition 3.9. These integrals over $[0, 1]^n$ are suitable to be evaluated using black-box integration algorithms. We implemented this in **Julia**, using the package **Polymake.jl** (v0.6.1) for polyhedral computations; see [6, 9] and [5]. Moreover, specializing to $h = 1$ in this representation of (11) gives a method for computing the normalization factor $\mathcal{I}^{\text{tr}} = \sum_{\sigma \in \mathcal{F}(n)} \mathcal{I}_{\sigma}^{\text{tr}}$ in Equation (14).

Remark 3.11. The sector decomposition (24) gives an alternative proof of Theorem 2.5, with no reference to [12]. A tropical study of the Mellin transform would be interesting. \diamond

Proposition 3.9 also gives the desired algorithm to sample from the tropical probability distribution in (14). As input we need the simplicial fan \mathcal{F} , where each maximal cone σ comes with the following data: a generating set, the vector δ_{σ} that encodes the function $f^{\text{tr}}/g^{\text{tr}}$ as in Lemma 3.7, and the numbers $\mathcal{I}_{\sigma}^{\text{tr}}$ in (19). Hence we also know $\mathcal{I}^{\text{tr}} = \sum_{\sigma \in \mathcal{F}(n)} \mathcal{I}_{\sigma}^{\text{tr}}$.

Algorithm 3.12 (Sampling from the tropical density $d_{f,g}^{\text{tr}}$).

Input: $\mathcal{F}(n)$, δ_{σ} , $\mathcal{I}_{\sigma}^{\text{tr}}$ and \mathcal{I}^{tr} .

1. Draw an n -dimensional cone σ from $\mathcal{F}(n)$ with probability $\mathcal{I}_{\sigma}^{\text{tr}}/\mathcal{I}^{\text{tr}}$.
2. Draw a sample q from the unit hypercube $[0, 1]^n$ using the uniform distribution.

3. Compute $x^\sigma(q) \in \text{Exp}(\sigma)$ with $x^\sigma(q)$ as in Proposition 3.9.

Output: The element $x^\sigma(q) \in X_{>0}$, a sample from the probability space $(X_{>0}, \mu_{f,g}^{\text{tr}})$.

The vector δ_σ and the generators of σ enter in the definition of the function $x^\sigma(q)$ in step 3. To show the correctness of Algorithm 3.12, consider any bounded test function $\psi : X_{>0} \rightarrow \mathbb{R}$. By Proposition 3.9, the expected value of the function $(\sigma, q) \mapsto \psi(x^\sigma(q))$ on $\mathcal{F}(n) \times [0, 1]^n$, where σ and q are sampled according to steps 1 and 2, is

$$\sum_{\sigma \in \mathcal{F}(n)} \frac{\mathcal{I}_\sigma^{\text{tr}}}{\mathcal{I}^{\text{tr}}} \int_{[0,1]^n} \psi(x^\sigma(q)) \, dq_1 \wedge \cdots \wedge dq_n = \frac{1}{\mathcal{I}^{\text{tr}}} \sum_{\sigma \in \mathcal{F}(n)} \int_{\text{Exp}(\sigma)} \frac{f^{\text{tr}}(x)}{g^{\text{tr}}(x)} \psi(x) \, \Omega_X.$$

We conclude from Equation (14) that the sum on the right is equal to the desired expectation

$$\mathbb{E}_{\mu_{f,g}^{\text{tr}}}[\psi] = \int_{X_{>0}} \psi(x) \mu_{f,g}^{\text{tr}} = \int_{X_{>0}} \psi(x) d_{f,g}^{\text{tr}} \Omega_X = \frac{1}{\mathcal{I}^{\text{tr}}} \int_{X_{>0}} \psi(x) \frac{f^{\text{tr}}(x)}{g^{\text{tr}}(x)} \Omega_X.$$

To run Algorithm 3.12 efficiently, we assume that the simplicial refinement \mathcal{F} of the normal fan of $\mathcal{N}(fg)$ has been precomputed offline. That computation can be time-consuming. In the application to statistics, cf. Section 6, this is done only once for any fixed model.

Step 1 of Algorithm 3.12 requires to sample from a finite set $\mathcal{F}(n)$ with a given probability distribution. With some preprocessing (cf. [18]), this task can be performed in a runtime which is independent of the cardinality of $\mathcal{F}(n)$. The runtime of the algorithm is therefore independent of the size of the fan \mathcal{F} , and it depends only linearly on the dimension n of X .

4 Numerical Integration and Rejection Sampling

In the previous section, we computed the tropical integral \mathcal{I}^{tr} and we explained how to sample from the tropical density. This will now be utilized in a non-tropicalized context. The domain of integration is the positive toric variety $X_{>0}$. We denote by $\mu_{f,g}$ the measure

$$\mu_{f,g} := \frac{1}{\mathcal{I}} \frac{f}{g} \Omega_X, \quad \text{where} \quad \mathcal{I} = \int_{X_{>0}} \frac{f}{g} \Omega_X. \quad (25)$$

We assume that the polynomials f and g satisfy the convergence criteria from Theorem 2.5. Similarly to that in Equation (15), the following function is a probability density on $X_{>0}$:

$$d_{f,g} := \frac{1}{\mathcal{I}} \cdot \frac{f}{g}. \quad (26)$$

Note that $\mu_{f,g} = d_{f,g} \cdot \Omega_X$. We regard $(X_{>0}, \mu_{f,g})$ as the classical version of the tropical probability space $(X_{>0}, \mu_{f,g}^{\text{tr}})$ which was introduced in Equation (14). The normalizing constant \mathcal{I} in (25) is the classical integral we saw in Equations (11) and (12). The classical and tropical probability measures $\mu_{f,g}$ and $\mu_{f,g}^{\text{tr}}$ are related to each other by the formula

$$\mu_{f,g} = \frac{\mathcal{I}^{\text{tr}}}{\mathcal{I}} \cdot h \cdot \mu_{f,g}^{\text{tr}}. \quad (27)$$

This section contains two novel contributions. We first present a tropical Monte Carlo method for numerically evaluating \mathcal{I} , and we then develop an algorithm for sampling from the density $d_{f,g}$ in (26). Applications to statistics will be featured in Sections 5 and 6.

We shall evaluate \mathcal{I} using the formula in (14), that is, by computing the expected value

$$\mathbb{E}_{\mu_{f,g}^{\text{tr}}}[h] = \int_{X_{>0}} h \mu_{f,g}^{\text{tr}} \quad (28)$$

with respect to the tropical measure $\mu_{f,g}^{\text{tr}}$ on the positive toric variety $X_{>0}$.

Corollary 4.1. *Suppose that Algorithm 3.12 is used to draw N i.i.d. samples $x^{(1)}, \dots, x^{(N)}$ from the space $X_{>0}$ with its tropical density. Then our integral (11) approximately equals*

$$\mathcal{I} \approx \mathcal{I}_N = \frac{\mathcal{I}^{\text{tr}}}{N} \sum_{i=1}^N h(x^{(i)}). \quad (29)$$

To assess the quality of this approximation, we first observe that Proposition 3.1 implies bounds in terms of the coefficients f_ℓ and g_ℓ of the given polynomials f and g . We have

$$M_1 \leq h(x) \leq M_2 \quad \text{for all } x \in X_{>0}, \quad (30)$$

where

$$M_1 = \frac{\min_{\ell \in \text{supp}(f)} f_\ell}{\sum_{\ell \in \text{supp}(g)} g_\ell} \quad \text{and} \quad M_2 = \frac{\sum_{\ell \in \text{supp}(f)} f_\ell}{\min_{\ell \in \text{supp}(g)} g_\ell}. \quad (31)$$

Proposition 4.2. *The standard deviation of the approximation in (29) is bounded by*

$$\sqrt{\mathbb{E}[(\mathcal{I} - \mathcal{I}_N)^2]} \leq \mathcal{I}^{\text{tr}} \cdot \sqrt{\frac{M_2^2 - M_1^2}{N}}. \quad (32)$$

Proof. The expected value of the random variable \mathcal{I}_N from (29) equals \mathcal{I} . It also equals $\mathcal{I}^{\text{tr}} \cdot \mathbb{E}_{\mu_{f,g}^{\text{tr}}}[h]$ by linearity. By the linearity of the variance for independent random variables,

$$\mathbb{E}[(\mathcal{I} - \mathcal{I}_N)^2] = \text{Var}[\mathcal{I}_N] = \left(\frac{\mathcal{I}^{\text{tr}}}{N}\right)^2 \text{Var}[h(x^{(1)}) + \dots + h(x^{(N)})] = \frac{(\mathcal{I}^{\text{tr}})^2}{N} \text{Var}[h].$$

Using the bounds in (30), we find that $\text{Var}[h] = \mathbb{E}[h^2] - \mathbb{E}[h]^2 \leq M_2^2 - M_1^2$. \square

Proposition 4.4 ensures that the method in Corollary 4.1 correctly computes a numerical approximation of the integral \mathcal{I} . The variance stays bounded and does not depend on $n = \dim(X)$. Another application of the tropical approach in Algorithm 3.12 is drawing from the probability density $d_{f,g}$ via *rejection sampling*. In the next paragraph, we briefly review the overall principle of rejection sampling. For further reading we refer to [7, Section 10.3].

Let d_1 and d_2 be densities on the same space with respect to the same differential form (e.g. $X_{>0}$ with Ω_X). Suppose it is hard to sample from d_1 , but sampling from d_2 is easy, and we know a constant $C \geq 1$ such that $d_1(x)/d_2(x) \leq C$ for all x in the domain. Our aim is to sample from d_1 using samples from d_2 . For this, we draw a sample x using the

distribution d_2 and a sample ξ from the interval $[0, C]$ with uniform distribution. We accept x if $\xi < d_1(x)/d_2(x)$. Otherwise, we reject x . The density of producing an accepted sample from this process is $d_2(x) \cdot d_1(x)/d_2(x)$. So, accepted samples follow the density d_1 .

We now apply rejection sampling to our problem. This is done as follows. The two densities of interest are $d_1 = d_{f,g}$ and $d_2 = d_{f,g}^{\text{tr}}$. From Equation (30), we obtain the inequality

$$d_{f,g} \leq \frac{\mathcal{I}^{\text{tr}}}{\mathcal{I}} \cdot M_2 \cdot d_{f,g}^{\text{tr}}. \quad (33)$$

We thus choose $C = (\mathcal{I}^{\text{tr}}/\mathcal{I}) \cdot M_2$ as our constant for rejection sampling. This suggests that rejection sampling requires to compute the integral \mathcal{I} . However, it is easy to check that if ξ is sampled uniformly from $[0, C]$, then $\xi' = (\mathcal{I}/\mathcal{I}^{\text{tr}}) \cdot \xi$ is sampled uniformly from $[0, M_2]$ and $\xi < d_{f,g}(x)/d_{f,g}^{\text{tr}}(x)$ is equivalent to $\xi' < h(x)$. This leads to the following algorithm.

Algorithm 4.3 (Sampling from the density $d_{f,g}$).

Input: The input from Algorithm 3.12 and the constant M_2 .

1. Draw a sample x from $X_{>0}$ using the tropical density $d_{f,g}^{\text{tr}}$.
2. Draw a sample ξ from the interval $[0, M_2]$ using the uniform distribution.
3. If $\xi < h(x)$, output x . Otherwise reject the sample and start again.

Output: The element $x \in X_{>0}$, a sample from the probability space $(X_{>0}, \mu_{f,g})$.

To check the validity of this algorithm, consider a bounded test function $\psi : X_{>0} \rightarrow \mathbb{R}$. The expected value of ψ , using the samples produced by Algorithm 4.3, is equal to

$$\mathbb{E}[\psi] = \frac{1}{D} \int_{X_{>0} \times [0, M_2]} \psi(x) H(h(x) - \xi) \mu_{f,g}^{\text{tr}} \wedge d\xi.$$

Here D is a normalization factor that ensures $\mathbb{E}[1] = 1$, and H denotes the *Heaviside function*, i.e., $H(t) = 0$ for $t \leq 0$ and $H(t) = 1$ for $t > 0$. By Equation (30), we have $h(x) \leq M_2$ for all $x \in X_{>0}$. Therefore, by evaluating the inner integral over ξ first, we obtain

$$\mathbb{E}[\psi] = \frac{1}{D} \int_{X_{>0}} \psi(x) h(x) \mu_{f,g}^{\text{tr}} = \frac{1}{D} \int_{X_{>0}} \psi(x) \frac{f}{g} \Omega_X.$$

This shows that $D = \mathcal{I}$, and we conclude that the expected value $\mathbb{E}[\psi]$ equals $\mathbb{E}_{\mu_{f,g}}[\psi]$.

The expected runtime of Algorithm 4.3 is equal to the runtime of Algorithm 3.12 divided by the *acceptance rate*. The latter is the probability that a sample drawn from $d_{f,g}^{\text{tr}}$ results in a valid sample for $d_{f,g}$. The bounds on h in (30) give rise to a lower bound for this probability.

Proposition 4.4. *The acceptance rate in Algorithm 4.3 is at least M_1/M_2 .*

Proof. The probability for acceptance of a sample equals

$$\frac{1}{M_2} \int_{X_{>0} \times [0, M_2]} H(h(x) - \xi) \mu_{f,g}^{\text{tr}} \wedge d\xi = \frac{1}{M_2} \cdot \int_{X_{>0}} h(x) \mu_{f,g}^{\text{tr}} \geq \frac{1}{M_2} \cdot M_1.$$

Here we used the lower bound from Equation (30). \square

The practical significance of Proposition 4.4 comes from the fact that the lower bound does not depend on the dimension n of the sample space $X_{>0}$. This guarantees that—even for high-dimensional problems—the acceptance rate in Algorithm 4.3 remains strictly positive.

We conclude with an example that illustrates the material presented in this section.

Example 4.5 (Pentagon). Let X be the toric surface in Example 2.2. We consider the integral \mathcal{I} in (25) and the probability density $d_{f,g}$ in (26) defined by the two positive polynomials

$$\begin{aligned} f &= 2x_1^2x_2^2x_3^3x_4x_5^3 + 3x_1^2x_2x_3^2x_4^2x_5^4 + 5x_1x_2^2x_3^5x_4x_5^2, \\ g &= 7x_1^3x_2^3x_3^2x_5^3 + 11x_1^3x_2x_4^2x_5^5 + 13x_1x_3^3x_4^3x_5^4 + 17x_2^2x_3^7x_4x_5. \end{aligned}$$

Both f and g are homogeneous of degree $\gamma = (3, 8, 8)$ in the grading given by (9). We remark that $\gamma \in \text{Cl}(X) \setminus \text{Pic}(X)$ does not come from a Cartier divisor. The 16 monomials of that degree are the lattice points in a quadrilateral whose normal fan is refined by Σ . This is shown in green in Figure 2. We see that the orange triangle $\mathcal{N}(f)$ is contained in the interior of the purple quadrilateral $\mathcal{N}(g)$. Hence Theorem 2.5 ensures that the integral \mathcal{I} converges.

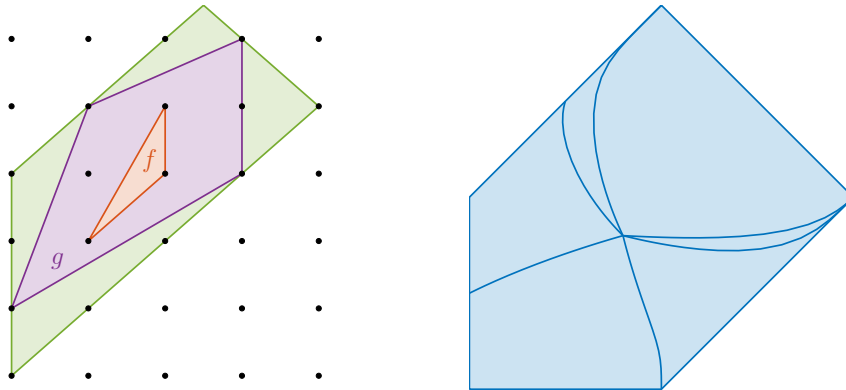


Figure 2: Newton polygons and sector decomposition from Example 4.5.

Let \mathcal{F} be the normal fan of the hexagon $\mathcal{N}(f) + \mathcal{N}(g)$. The tropical integral \mathcal{I}^{tr} is the sum of the six rational numbers $\mathcal{I}_{\sigma}^{\text{tr}}$ in (19). Here σ is one of the six cones in $\mathcal{F}(2)$. We find

$$\mathcal{I}^{\text{tr}} = 1 + 2 + \frac{3}{2} + 1 + \frac{1}{4} + \frac{7}{2} = \frac{37}{4}.$$

The surface $X_{>0}$ is divided into six sectors $\text{Exp}(\sigma)$. This division can be visualized via the moment map $X_{>0} \rightarrow P^{\circ}$, as shown in Figure 2. On each sector, we have a monomial map $q \mapsto x^{\sigma}(q)$ with rational exponents, given explicitly in Equation (22). Using this map, we now apply Algorithm 3.12 as follows. We draw $N = 10000$ samples from the tropical density $d_{f,g}^{\text{tr}}$. The formula (29) then gives the following approximate value for the classical integral:

$$\mathcal{I} \approx 2.8677596477559826.$$

We now apply Proposition 4.2. Using (31), we find $M_1 = 1/24$ and $M_2 = 10/7$. This implies that the standard deviation $\sqrt{\mathbb{E}[(\mathcal{I} - \mathcal{I}_N)^2]}$ is at most 0.132. By comparing with a

more accurate approximation, using numerical cubature for (21), we find that the error is no larger than 0.005. Repeating this experiment for a range of sample sizes N , we find that our approximation beats the generic bound (32) by two orders of magnitude. This illustrates a phenomenon that is observed for many examples: the bounds (32) are overly pessimistic.

Finally, we use Algorithm 4.3 to sample from the posterior distribution $d_{f,g}$. Using $N = 100000$ candidate samples, we find that 21808 are accepted. The bound on the expected value of the acceptance rate in Proposition 4.4 is $M_1/M_2 \approx 0.03$. Again, this is pessimistic. Indeed, from the proof of Proposition 4.4 we see that the actual expected acceptance rate is

$$\frac{1}{M_2} \cdot \frac{\mathcal{I}}{\mathcal{I}^{\text{tr}}} \approx 0.22. \quad \diamond$$

5 Statistical Models

In this section, we present several statistical models, some well-known and others less so. They all have a natural polyhedral structure which allows for a parameterization $X_{>0} \rightarrow \Delta_m$. This includes both toric models and linear models. We argue that this passage to toric geometry makes sense, also from an applied perspective, since Bayesian integrals (36) can now be evaluated using tropical sampling. Such integrals depend on the data u_0, \dots, u_m . We will study them in the next section. We here consider the models but not yet the data.

The common parameter space for our models is the positive part of an n -dimensional projective toric variety $X = X_\Sigma$. We assume that the fan Σ is simplicial, so it is the normal fan of a simple lattice polytope P in \mathbb{R}^n . The polytope P is not unique. There is one such polytope for each very ample divisor on X . The vertex set $\mathcal{V}(P)$ is in bijection with the maximal cones in the normal fan of P . The prior distribution on $X_{>0}$ has a density that is a positive rational function. We obtain 1 when integrating this density against the form

$$\Omega_X = \sum_I \det(V_I) \bigwedge_{i \in I} \frac{dx_i}{x_i}. \quad (34)$$

Fix the uniform distribution on the polytope P . We shall consider models of the form

$$P \rightarrow \Delta_m, \quad y \mapsto (p_0(y), p_1(y), \dots, p_m(y)). \quad (35)$$

One task in Section 6 is to evaluate marginal likelihood integrals with uniform priors on P :

$$\int_P p_0^{u_0} p_1^{u_1} \cdots p_m^{u_m} \, dy_1 \wedge \cdots \wedge dy_n. \quad (36)$$

One still needs to divide by the volume of P . We here ignore this factor for simplicity.

We lift (35) to the positive toric variety $X_{>0}$ by composing with the moment map $X_{>0} \rightarrow P^\circ$, where P° is the interior of P . We do this in two steps, by writing the moment map as $\varphi \circ \phi$, where ϕ is the identification $X_{>0} \simeq \mathbb{R}_{>0}^n$ and $\varphi : \mathbb{R}_{>0}^n \rightarrow P^\circ$ is the *affine moment map*. The latter can be defined by a Laurent polynomial with positive coefficients $c_a \in \mathbb{R}_{>0}$,

$$q = \sum_{a \in \mathcal{V}(P)} c_a t^a \in \mathbb{R}[t_1^{\pm 1}, \dots, t_n^{\pm 1}].$$

The map φ sends $t \in \mathbb{R}_{>0}^n$ to the following convex combination of $\mathcal{V}(P)$:

$$\varphi(t) = \frac{1}{q(t)} (\theta_1(q(t)), \dots, \theta_n(q(t))) = \sum_{a \in \mathcal{V}(P)} \frac{c_a t^a}{q(t)} \cdot a. \quad (37)$$

Here, θ_i denotes the i th Euler operator $t_i \partial_{t_i}$. The *toric Jacobian* $(\theta_j(\varphi_i))_{i,j}$ of the map φ is the *toric Hessian* H of $\log(q(t))$. This is the symmetric $n \times n$ matrix with entries $H_{i,j} = \theta_i \theta_j (\log q(t))$. Since φ is a diffeomorphism, the determinant of H is nowhere zero on $\mathbb{R}_{>0}^n$. Moreover, its denominator q^n has positive coefficients, so there are no poles on $\mathbb{R}_{>0}^n$ either. Recall that the columns of $V \in \mathbb{Z}^{n \times k}$ are the facet normals of the simple polytope P . This gives us a formula for the density on $X_{>0}$ that represents the uniform distribution on P .

Proposition 5.1. *The pullback of $dy_1 \cdots dy_n$ under the moment map $X_{>0} \rightarrow P^\circ$ is a positive rational function r times the canonical form Ω_X . We obtain $r(x)$ from the toric Hessian $H(t)$ by replacing t_1, \dots, t_n with the Laurent monomials in x_1, \dots, x_k given by the rows of V .*

Example 5.2. Consider the coin model in the Introduction, with $n = 3$, $P = [0, 1]^3$, and $X = \mathbb{P}^1 \times \mathbb{P}^1 \times \mathbb{P}^1$. The desired rational function r is the factor before Ω_X in Equation (4). \diamond

Proposition 5.1 means that the integral (36) is equal to the following integral over $X_{>0}$:

$$\int_{X_{>0}} p_0(x)^{u_0} p_1(x)^{u_1} \cdots p_m(x)^{u_m} r(x) \Omega_X, \quad (38)$$

where $p_i(x)$ is obtained from $p_i(y)$ by the two-step substitution described above, i.e., we first set $y = \varphi(t)$ and then we replace t with the Laurent monomials in x given by the rows of V .

Example 5.3. We revisit the pentagon P from Example 2.2. It is the Newton polytope of

$$q(t_1, t_2) = t_2^{-1} + t_1^{-1} t_2^{-1} + t_1^{-1} + t_2 + t_1.$$

We identify its interior P° with the positive quadrant $\mathbb{R}_{>0}^2$ via the affine moment map

$$\varphi: \mathbb{R}_{>0}^2 \xrightarrow{\sim} P^\circ, \quad (t_1, t_2) \mapsto \frac{1}{q} (\theta_1(q), \theta_2(q)).$$

Its toric Jacobian is the toric Hessian H of $\log(q)$. Its determinant is

$$\det(H) = (t_1 t_2)^{-2} (4t_1^3 t_2^2 + 4t_1^2 t_2^3 + 9t_1^2 t_2^2 + 4t_1^2 t_2 + 4t_1 t_2^2 + t_1^2 + 8t_1 t_2 + t_2^2 + 1) \cdot q(t_1, t_2)^{-3}.$$

Turning the rows of (8) into monomials, we now set $t_1 = x_1 x_2 x_3^{-1} x_4^{-1}$ and $t_2 = x_2^{-1} x_3^{-1} x_4 x_5$. This substitution turns $\det(H)$ into the rational function r , as seen in Proposition 5.1. Writing $r = f/g$ as in Theorem 2.5, one checks that the two Newton polygons satisfy the containment hypothesis. It is instructive to check by computing the area of the pentagon:

$$\int_{X_{>0}} r(x) \Omega_X = \int_P 1 dy_1 dy_2 = \frac{5}{2}.$$

The integrals are (38) = (36) with $u_i = 0$. The first is evaluated numerically by Section 4. \diamond

We now introduce the *linear model* associated with our polytope P . From now on we assume that P contains the origin in its interior. Then we have the inequality representation

$$P = \{ y \in \mathbb{R}^n \mid \langle v_i, y \rangle + \alpha_i \geq 0 \text{ for } i = 1, 2, \dots, k \},$$

where $\alpha_1, \dots, \alpha_k$ are positive integers. Vertices q_I of P are indexed by cones $I \in \Sigma(n)$. The vertex $q_I \in \mathbb{Z}^n$ is the unique solution to the n linear equations $\langle v_i, y \rangle = -\alpha_i$ for $i \in I$.

The states of the linear model are the k facets of P . The probability of the i -th facet is

$$p_i(y) = \frac{1}{\gamma_i} (\alpha_i + \langle v_i, y \rangle), \quad (39)$$

where the $\gamma_i > 0$ are chosen so that $p_1(y) + \dots + p_k(y) = 1$. The probabilities are nonnegative precisely on the polytope P . The linear model is the image of the resulting map $P \rightarrow \Delta_{k-1}$.

While the states in the linear model are the facets of our simple polytope P , we now introduce a variant where the vertices y_I serve as the states. Their number is $m+1 = |\Sigma(n)|$.

The following polynomial in n unknowns is known as the *adjoint* of the polytope P :

$$A(y) = \sum_{I \in \Sigma(n)} |\det(\tilde{V}_I)| \cdot \prod_{i \notin I} \left(1 + \frac{1}{\alpha_i} \langle v_i, y \rangle \right).$$

In the formula above, the matrix \tilde{V} is obtained from V by scaling the i th column with α_i^{-1} . This formula looks like the canonical form Ω_X on the toric variety X . Namely, we replace x_i in (34) by the i -th facet equation and we clear denominators. More precisely, the following differential form on P is the pushforward of Ω_X under the moment map $X_{>0} \rightarrow P$ above:

$$\Omega_P = \frac{A}{\prod_{i=1}^k \left(1 + \frac{1}{\alpha_i} \langle v_i, y \rangle \right)} dy_1 \cdots dy_n.$$

Arkani-Hamid, Bai, and Lam [1, Theorem 7.2] proved that Ω_P is the canonical form of the pair (\mathbb{P}^n, P) . Thus, the adjoint A endows P with the structure of a positive geometry.

Each summand of A has degree $k - n$, but the adjoint has degree $k - n - 1$, because the highest degree terms cancel. Consider the summand indexed by the cone $I \in \Sigma(n)$:

$$p_I(y) = \frac{|\det(\tilde{V}_I)|}{A(y)} \prod_{i \notin I} \left(1 + \frac{1}{\alpha_i} \langle v_i, y \rangle \right). \quad (40)$$

These products of $k - n$ affine-linear forms satisfy the following remarkable identities:

$$\sum_{I \in \Sigma(n)} p_I(y) = 1 \quad \text{and} \quad \sum_{I \in \Sigma(n)} p_I(y) q_I = y.$$

These identities tell us that the $p_I(y)$ serve as barycentric coordinates on P . They express each point y in the polytope P canonically as a convex combination of the $m+1$ vertices q_I . The resulting statistical model with state space $\Sigma(n)$ is known as the *Wachspress model*:

$$P \longrightarrow \Delta_m, \quad y \mapsto (p_I(y))_{I \in \Sigma(n)}.$$

Example 5.4 (Pentagon). The pentagon in Example 2.2 matches [1, Figure 8]. Here, $n = 2$, $k = m + 1 = 5$, and P is defined by requiring that the following expressions are nonnegative:

$$\ell_1 = 1 + y_1, \quad \ell_2 = 1 + y_1 - y_2, \quad \ell_3 = 1 - y_1 - y_2, \quad \ell_4 = 1 - y_1 + y_2, \quad \ell_5 = 1 + y_2. \quad (41)$$

Here, P was shifted so that the interior point in Figure 1 is the origin. The vertices are

$$y_{12} = (-1, 0), \quad y_{23} = (0, 1), \quad y_{34} = (1, 0), \quad y_{45} = (0, -1), \quad y_{51} = (-1, -1).$$

The linear model given by the map $P \rightarrow \Delta_4$, $y \mapsto \frac{1}{5}(\ell_1(y), \dots, \ell_5(y))$. Its states are the five edges of the pentagon P . The distributions in this model are the points $p \in \Delta_4$ that satisfy

$$2p_1 - 2p_2 + p_3 - p_4 = -p_2 - 2p_4 + p_3 + 2p_5 = 0.$$

We next describe the Wachspress model. The adjoint of P is the quadratic polynomial

$$A = 7 + 2(y_1 + y_2) - (y_1 - y_2)^2 = \ell_1\ell_2\ell_3 + \ell_2\ell_3\ell_4 + \ell_3\ell_4\ell_5 + 2\ell_4\ell_5\ell_1 + 2\ell_5\ell_1\ell_2.$$

The states of the model are the five vertices of the pentagon P . Their probabilities are

$$(p_{45}, p_{51}, p_{12}, p_{23}, p_{34}) = \frac{1}{A}(\ell_1\ell_2\ell_3, \ell_2\ell_3\ell_4, \ell_3\ell_4\ell_5, 2\ell_4\ell_5\ell_1, 2\ell_5\ell_1\ell_2). \quad (42)$$

Each p_{ij} is a rational function with cubic numerator and quadratic denominator. This defines the Wachspress model $P \rightarrow \Delta_4$. Distributions in the model are points $p \in \Delta_4$ that satisfy

$$2p_{12}p_{45} + 2p_{23}p_{45} - p_{23}p_{51} - 2p_{34}p_{51} = 2p_{12}p_{34} - 2p_{23}p_{45} - p_{23}p_{51} + p_{34}p_{51} = 0.$$

Geometrically, this is a del Pezzo surface of degree four in \mathbb{P}^4 , obtained by blowing up \mathbb{P}^2 at five points. These points are the intersections of pairs of edge lines that are not in P . \diamond

We now turn to *toric models*. In algebraic statistics [15], these are described as models parameterized by monomials. We here recast them in the setting of Section 2. Fix a degree $\gamma \in \text{Cl}(X)$ and let $Z \in S$ be a homogeneous polynomial of degree γ with positive coefficients,

$$Z = c_0x^{a_0} + c_1x^{a_1} + \dots + c_mx^{a_m}.$$

We divide each of the summands by Z to get rational functions p_i of degree zero on X :

$$p_i = \frac{c_i x^{a_i}}{Z}, \quad \text{for } i = 0, 1, \dots, m.$$

These functions are positive on $X_{>0}$ and their sum is equal to 1. The toric model of Z is the resulting map $X_{>0} \rightarrow \Delta_m$ into the probability simplex. In this manner, we identify toric models on X with homogeneous positive polynomials Z in the Cox ring $S_{\mathbb{R}} = \mathbb{R}[x_1, \dots, x_k]$.

The model is especially nice when the degree γ is very ample and Z uses all monomials of degree γ . In that case, the Newton polytope $P = \mathcal{N}(Z)$ is simple and its normal fan is the fan of X . In symbols, we have $\mathcal{F} = \Sigma$, which is a favorable situation for tropical sampling.

Example 5.5. Let γ be the very ample degree associated with the pentagon in Example 2.2. A general polynomial of degree γ has six monomials, one for each lattice point in Figure 1:

$$Z = c_0 x_2 x_3^3 x_4 + c_1 x_1 x_2^2 x_3^2 + c_2 x_3^2 x_4^2 x_5 + c_3 x_1 x_2 x_3 x_4 x_5 + c_4 x_1^2 x_2^2 x_5 + c_5 x_1 x_4^2 x_5^2. \quad (43)$$

The toric model is the map $X_{>0} \rightarrow \Delta_5$ given by the six terms. Geometrically, up to scaling the coordinates by the $c_i > 0$, this is the projective embedding of X into \mathbb{P}^5 given by γ . \diamond

Remark 5.6. Let P be a product of standard simplices, so X is a product of projective spaces. For $\gamma = (1, 1, \dots, 1)$, $\mathcal{O}(\gamma)$ is the very ample line bundle of the Segre embedding. Here, the toric model coincides with the Wachspress model. Each distribution in this model is a tensor of rank one [15, Section 16.3]. Its mixture models encode tensors of higher rank. \diamond

The setting of Section 2 is convenient for working with *mixture models* [15, Section 14.1]. Given any model $p : X_{>0} \rightarrow \Delta_m$, its r -th mixture model lives on the toric variety $X^r \times \mathbb{P}^{r-1}$. The parameter space $(X^r \times \mathbb{P}^{r-1})_{>0} = X_{>0}^r \times \mathbb{P}_{>0}^{r-1}$ is mapped into Δ_m by the secant map. Geometrically, the mixture model is the r th secant variety [15, Definition 14.1.5] of $\text{im}(p)$.

Mixture models of toric models play an important role in applications. Going beyond Remark 5.6, consider the model of symmetric tensors of nonnegative rank $\leq r$. In statistics, this is known as the model of conditional independence for identically distributed random variables. We refer to [10] for Bayesian integrals and to [14, Section 5] for likelihood inference.

The model in the Introduction is the $r = 2$ mixture of a toric model on $X = \mathbb{P}^1$. We conclude this section with a case study of this coin model from the perspective of Section 3.

The rational functions in (1) have distinct numerators P_0, \dots, P_m but the same denominator $Q = (x_0 + x_1)(s_0 + s_1)^m(t_0 + t_1)^m$. The Minkowski sum of their Newton polytopes,

$$\mathcal{N}(Q) + \mathcal{N}(P_0) + \mathcal{N}(P_1) + \dots + \mathcal{N}(P_m), \quad (44)$$

is a 3-dimensional polytope in \mathbb{R}^6 . Its normal fan \mathcal{F} , which lives in a quotient space $\mathbb{R}^6/\mathbb{R}^3$, is an essential ingredient for the algorithms in Sections 3 and 4. We now compute this.

Theorem 5.7. *The Newton polytope (44) has $8(m+1)$ vertices, $14m+12$ edges and $6(m+1)$ facets. Each of the eight vertices of the cube $\mathcal{N}(Q)$ is a summand of $m+1$ vertices. Among the $6(m+1)$ facets, four are pentagons, two are $2(m+1)$ -gons and the rest are quadrilaterals.*

Sketch of Proof. Consider a generic vector w in \mathbb{R}^6 that assigns weights to the six Cox coordinates. The leading monomial $x_i s_j^m t_k^m$ of Q is determined by the signs of the quantities

$$w(x_0) - w(x_1), \quad w(s_0) - w(s_1), \quad w(t_0) - w(t_1). \quad (45)$$

We record this leading monomial in the binary string ijk . Each of these eight choices allows for $m+1$ consistent choices of leading monomials from the tuple (P_0, P_1, \dots, P_m) . Indeed, the leading monomial of P_ℓ coincides with that of the binomial $\tilde{P}_\ell = x_0 s_0^\ell s_1^{m-\ell} t_0^m + x_1 t_0^\ell t_1^{m-\ell} s_0^m$. The line segments $\mathcal{N}(\tilde{P}_\ell)$ lie in translates of a common 2-dimensional subspace in \mathbb{R}^6 , and their Minkowski sum is a $(2m+2)$ -gon. Precisely half of its vertices are compatible with the inequalities (45). These $m+1$ vertices become vertices of (44), and they are all the vertices.

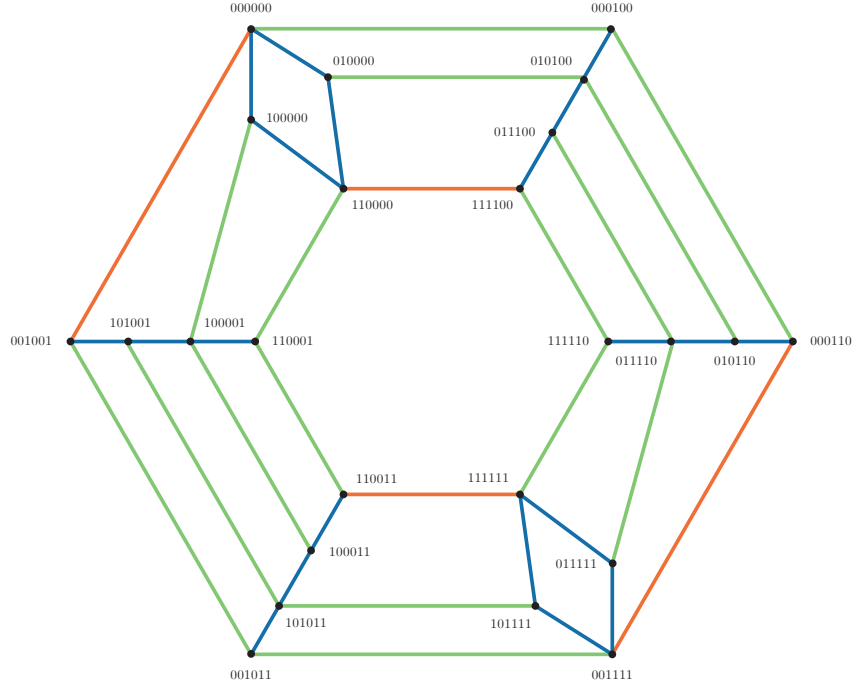


Figure 3: Schlegel diagram of the polytope (44) for $m = 2$. The 24 vertices are labeled by binary strings. There are four special edges (orange) and 36 regular ones: 16 of class 1 (green) and 20 of class 2 (blue). Among the 18 facets, we see two hexagons and two pentagons.

We encode each vertex of (44) by a binary string of length $m + 4$, starting with ijk . The other $m + 1$ entries indicate the leading terms of the P_ℓ . Namely, we write 0 if the expression

$$w(x_0) - w(x_1) + (m - \ell)(w(s_1) - w(s_0)) + (m - \ell)(w(t_0) - w(t_1))$$

is positive, and we write 1 if it is negative. With this notation, here are all $8(m + 1)$ vertices:

$$\begin{aligned} 0001^\ell 0^{m-\ell+1}, \quad 0101^\ell 0^{m-\ell+1}, \quad 1000^\ell 1^{m-\ell}, \quad 1100^\ell 1^{m-\ell}, \\ 0010^\ell 1^{m-\ell+1}, \quad 1010^\ell 1^{m-\ell+1}, \quad 0111^\ell 1^{m-\ell}, \quad 1111^\ell 1^{m-\ell}, \end{aligned} \quad \text{for } \ell = 0, 1, \dots, m.$$

Any pair of such strings that differs in precisely one entry is an edge of (44). This accounts for all but four of the edges. These special edges are pairs of strings that differ in two positions:

$$[0000^{m+1}, 0010^m] \quad [0001^m 0, 0011^{m+1}] \quad [1100^{m+1}, 1110^m] \quad [11001^m, 1111^{m+1}].$$

The other $14m + 8$ *regular edges* come in two classes. In the first class, the initial triple ijk in the binary string is fixed. For each initial triple ijk there are m such edges, for a total of $8m$ edges. The remaining $6m + 8$ edges correspond to a sign change in $w(x_0) - w(x_1)$, $w(s_0) - w(s_1)$ or $w(t_0) - w(t_1)$. Here, the terminal $m + 1$ letters in the binary string is fixed. If that string is 0^{m+1} or 1^{m+1} then there are four edges which form a square facet of our polytope, namely the square $000^{m+2}, 010^{m+2}, 110^{m+2}, 100^{m+2}$, 000^{m+2} and the square $001^{m+2}, 011^{m+2}, 111^{m+2}, 101^{m+2}, 001^{m+2}$. For each of the other $2m$ terminal strings, there

are only three edges which form a 3-chain, for instance $0010^m 1$, $1010^m 1$, $1000^m 1$, $1100^m 1$. This accounts for all $4 + 8 \cdot m + (4 + 4) + (2m) \cdot 3 = 14m + 12$ edges of our polytope (44).

We now discuss the $6m + 6$ facets. First, there are two centrally symmetric $2(m+1)$ -gons. They are formed by all strings that start with 00 or 11 respectively. There are precisely two other facets adjacent to both $2(m+1)$ -gons, namely the two squares facets mentioned above. Adjacent to these two squares and to the two big facets are the four pentagons, which are

$$0000^{m+1}, 1000^{m+1}, 1000^m 1, 1010^m 1, 0010^m 1 \quad \text{and} \quad 0011^{m+1}, 0111^{m+1}, 0111^m 0, 0101^m 0, 0001^m 0, \\ 1111^{m+1}, 1011^{m+1}, 10101^m, 10001^m, 11001^m \quad \text{and} \quad 1100^{m+1}, 0100^{m+1}, 01010^m, 01110^m, 11110^m.$$

Each pentagon contains one of the four special edges. The remaining facets are quadrilaterals. They come in six strips of m facets. Our polytope for $m = 2$ is shown in Figure 3. \square

6 Marginal Likelihood Integrals

We now come to applications in Bayesian inference. We fix a statistical model $X_{>0} \rightarrow \Delta_m$ that is specified by $m+1$ rational functions p_i on the toric variety X . These rational functions sum to 1. We write $p_i(x) = q_i(x)/r_i(x)$, where the numerator q_i and the denominator r_i are homogeneous polynomials with positive coefficients that have the same degree in $\text{Cl}(X)$. We further assume that we are given a rational function f/g that defines a probability distribution $\mu_{f,g}$ on $X_{>0}$ as in (25). This serves as the prior distribution for Bayesian inference.

The data comes in the form of U samples from the state space $\{0, 1, \dots, m\}$. We write u_i for the number of samples that are in state i . We assume that the integers u_i are positive. They satisfy $u_0 + u_1 + \dots + u_m = U$. Given $u = (u_0, u_1, \dots, u_m)$, the *likelihood function* L_u is

$$L_u(x) := \frac{\prod_{i=0}^m q_i(x)^{u_i}}{\prod_{i=0}^m r_i(x)^{u_i}}. \quad (46)$$

This expression is the probability of observing the data vector u , assuming that the model, the parameters x , and the sample size U are fixed. The Multinomial Theorem implies that

$$\sum_{|u|=U} \frac{U!}{u_0! u_1! \dots u_m!} \cdot L_u(x) = 1 \quad \text{for all } x \in X_{>0}.$$

We are interested in the *posterior density* on $X_{>0}$. Up to a constant factor, this equals

$$d_u := L_u \cdot d_{f,g}. \quad (47)$$

The *marginal likelihood integral* \mathcal{I}_u is the integral of (46) against $\mu_{f,g}$, i.e.,

$$\mathcal{I}_u := \int_{X_{>0}} L_u(x) \mu_{f,g} = \frac{1}{\mathcal{I}} \int_{X_{>0}} L_u(x) \frac{f(x)}{g(x)} \Omega_X. \quad (48)$$

We shall evaluate \mathcal{I}_u using the methods in Section 4, but with f/g replaced by $L_u \cdot f/g$. Another task of interest is sampling from the posterior density d_u , by way of Algorithm 4.3.

The Newton polytope of the integrand $L_u \cdot f/g$ admits the Minkowski sum decomposition

$$\mathcal{N}(f) + \mathcal{N}(g) + \sum_{i=0}^m u_i \mathcal{N}(q_i) + \sum_{i=0}^m u_i \mathcal{N}(r_i). \quad (49)$$

The normal fan of this polytope is independent of the data u since u_0, \dots, u_m are positive. As before, we let \mathcal{F} be a simplicial refinement of the normal fan of the polytope in (49). We thus conclude the following fact, which is important for the applicability of our method.

Observation 6.1. *The simplicial fan \mathcal{F} is independent of the data u . It is computed from the statistical model. This is done in an offline step that is carried out only once per model.*

The computation of \mathcal{F} is expensive when the dimension n gets larger. Observation 6.1 means that the running time of the algorithms in Sections 3 and 4 is fairly independent of u . For instance, consider the computation of the sector integrals $\mathcal{I}_\sigma^{\text{tr}}$ using the formula in (19). The data u do not appear in the numerator, but they do enter in the denominator. Namely, the monomial $x^{-\delta_\sigma}$ that represents the tropicalized integrand $L_u^{\text{tr}} f^{\text{tr}}/g^{\text{tr}}$ on $\text{Exp}(\sigma)$ satisfies

$$\delta_\sigma = \nu_g - \nu_f + \sum_{i=0}^m u_i (\nu_{r_i} - \nu_{q_i}).$$

In an offline step, done once per model, we precompute the $k \times (m+1)$ matrix of inner products $w_\ell \cdot (\nu_{r_i} - \nu_{q_i})$. In the online step, with data u , we can then evaluate (19) rapidly.

One point that does depend on the data u is the accuracy of the approximation in (29). The bounds M_1 and M_2 for the function h scale exponentially in U , and hence so does the right hand side of (32). The quality of approximation \mathcal{I}_N can decrease a lot for larger U . We observed this phenomenon in our computations. This issue requires further study.

We now present computational experiments with the models we saw in Sections 1 and 5. This material is made available at [MathRepo](#) [5]. We encourage our readers to try it out. Our implementation is in [Julia](#) and it relies on [Polymake](#) [6] for polyhedral computations.

Example 6.2 (Coin model). Consider the coin model from the Introduction. We begin with $m = 2$. Fix $U = 5$ and the data vector $u = (u_0, u_1, u_2) = (2, 1, 2)$. The marginal likelihood integral (48) is a rational number. Using symbolic computation as in [10], we find the value

$$\mathcal{I}_u = \frac{2267}{1559250} \approx 0.001454.$$

We reproduce this number using tropical sampling. The Newton polytope (44) of the integrand is shown in Figure 3. Its normal fan has 24 maximal cones, one for each vertex. But, this fan is not simplicial since eight of the vertices are 4-valent. We turn (44) into a simple polytope by a small displacements of the facets. The resulting normal fan is simplicial, and it has $32 = 24 + 8$ maximal cones. That simplicial fan \mathcal{F} is used for the sector decomposition. The right hand side in (24) has 32 summands, one for each cone $\sigma \in \mathcal{F}(3)$. The values of the 32 tropical sector integrals $\mathcal{I}_\sigma^{\text{tr}}$ are the rational numbers $\frac{1}{280}, \frac{1}{280}, \frac{1}{280}, \frac{1}{280}, \frac{1}{120}, \dots, \frac{1}{8}, \frac{1}{7}, \frac{1}{7}$. Their sum equals $\mathcal{I}^{\text{tr}} = \frac{40}{21} = 1.9047$. This gives the discrete probability distribution used in Step 1 of Algorithm 3.12. Numerical evaluation of (29) with sample size $N = 50000$ yields

$$\mathcal{I}_N = 0.001486.$$

We validated our method with a range of experiments for larger values of U, m, N . \diamond

Example 6.3 (Pentagon models). We revisit the linear model and the Wachspress model from Example 5.4. Their common parameter space is the pentagon P with uniform prior. This is lifted to the toric surface $X_{>0}$ with density $d_{f,g}$ given by the homogeneous polynomials f and g in Example 5.3. The coordinates of the two models are obtained from the polynomials in y seen in Example 5.4. We first substitute $y_1 = \frac{t_1}{q} \frac{\partial q}{\partial t_1}$ and $y_2 = \frac{t_2}{q} \frac{\partial q}{\partial t_2}$, and then we set $t_1 = x_1 x_2 x_3^{-1} x_4^{-1}$ and $t_2 = x_2^{-1} x_3^{-1} x_4 x_5$. In each case, this yields a rational function $L_u f/g$ that is homogeneous of degree zero in x , and satisfies the hypothesis in Theorem 2.5.

The likelihood functions for the linear model and the Wachspress model look similar, but there is a crucial distinction. The latter also involves the adjoint A . This means that statistical inference is different for the two models. For instance, the ML degree of the linear model on P equals five, while the ML degree of the Wachspress model on P equals eight.

Consider the linear model with $(u_1, u_2, u_3, u_4, u_5) = (20, 16, 10, 15, 23)$. With (41) we have

$$\mathcal{I}_u = \frac{1}{5^{84}} \cdot \frac{2}{5} \cdot \int_P \ell_1^{20} \ell_2^{16} \ell_3^{10} \ell_4^{15} \ell_5^{23} dy_1 dy_2. \quad (50)$$

For the approximation by tropical sampling, we note that the Newton polygon of $L_u f/g$ has seven vertices, so its normal fan \mathcal{F} has $|\mathcal{F}(2)| = 7$. We find that $\mathcal{I}_u \approx 9.652 \cdot 10^{-60}$.

We now compare this with the Wachspress model, where we take the data vector to be $(u_{123}, u_{234}, u_{345}, u_{451}, u_{512}) = (2, 3, 5, 7, 11)$. Now the marginal likelihood integral equals

$$\mathcal{I}_u = 2^{13} \cdot \frac{2}{5} \cdot \int_P \ell_1^{20} \ell_2^{16} \ell_3^{10} \ell_4^{15} \ell_5^{23} A^{-84} dy_1 dy_2. \quad (51)$$

where $A = 7 + 2(y_1 + y_2) - (y_1 - y_2)^2$ is the adjoint. Again, the Newton polygon of $L_u f/g$ has seven vertices, so its normal fan \mathcal{F} has $|\mathcal{F}(2)| = 7$. We find that $\mathcal{I}_u \approx 1.218 \cdot 10^{-66}$. \diamond

We now illustrate how our techniques can be applied to Bayesian model selection.

Example 6.4 (Bayes factors). As before, let $\mu_{f,g}$ denote the prior arising from the toric Hessian. We consider the data $u = (u_0, u_1, \dots, u_5) = (1, 2, 4, 8, 16, 32)$. We wish to decide between two models with $n = 2$ and $m = 5$. The two competitors are toric models with p_i and Z as in Example 5.5, with different coefficient vectors $c = (c_0, c_1, \dots, c_5)$. Model \mathcal{M}_1 is given by $c^{(1)} = (2, 3, 5, 7, 11, 13)$ while model \mathcal{M}_2 is given by $c^{(2)} = (32, 16, 8, 4, 2, 1)$. We denote the respective likelihood functions by $L_u^{(1)}$ and $L_u^{(2)}$ and the marginal likelihood integrals by

$$\mathcal{I}_u^{(i)} = \int_{X_{>0}} L_u^{(i)}(x) \mu_{f,g}, \quad i = 1, 2.$$

In order to decide which model fits the data better, we compute the ratio $K = \mathcal{I}_u^{(1)} / \mathcal{I}_u^{(2)}$ of the two marginal likelihood integrals. This ratio is the *Bayes factor*. Using numerical cubature with tolerance $1e-5$, we find that $\mathcal{I}_u^{(1)} \approx 5.675 \cdot 10^{-38}$ and $\mathcal{I}_u^{(2)} \approx 2.694 \cdot 10^{-39}$. Therefore, $K \approx 21.06$, which reveals that the model \mathcal{M}_1 is a better fit for u than \mathcal{M}_2 . \diamond

Another important Bayesian application is sampling from the posterior distribution. In principle, this can be done with Algorithm 4.3, applied to the density d_u in (47). However, this fails to work as an off-the-shelf method. At present, the method is of theoretical interest

only. The challenge arises from large integer exponents, like 84 in Equation (51). These exponents lead to a very low acceptance rate in Proposition 4.4. We also observed this in practice: in a typical run of Algorithm 4.3 for (50) with $N = 100000$, all samples are rejected.

We conclude that our tropical sampling method rests on solid and elegant mathematical foundations, and it holds considerable promise for Bayesian inference. Yet, more research is needed to make it widely applicable for computational statistics. For larger sample size U , the likelihood function L_u has a sharp peak around its maximum, so it will be important to precompute the critical points of L_u . The algebraic complexity for this task is the ML degree of the model. This suggests combining tropical sampling with the topological theory of ML degrees. Our experiments also showed that exact symbolic algorithms (cf. [10]) are still surprisingly competitive. For instance, the exact value of the integral \mathcal{I}_u in (50) equals

$$\frac{139123 \cdot 1256291317 \cdot 2602507379 \cdot 47336895027767486610187}{2^4 \cdot 3^6 \cdot 5^{88} \cdot 7^2 \cdot 11 \cdot 13^2 \cdot 17^2 \cdot 19 \cdot 23^2 \cdot 29^2 \cdot 31^2 \cdot 37^2 \cdot 41^2 \cdot 43 \cdot 47 \cdot 53 \cdot 59 \cdot 61 \cdot 67 \cdot 71 \cdot 79 \cdot 83}.$$

In a future project, we plan to combine the methods of Sections 3 and 4 with exact evaluation.

Acknowledgments. We thank Thomas Lam for an insightful discussion on positive geometries. M. B. was supported by Dr. Max Rössler, the Walter Haefner Foundation, and the ETH Zürich Foundation.

References

- [1] N. Arkani-Hamed, Y. Bai, and T. Lam: Positive geometries and canonical forms, *J. High Energy Phys.* **11** (2017) 1–124.
- [2] M. Borinsky: Tropical Monte Carlo quadrature for Feynman integrals, *Annales de l’Institut Henri Poincaré D*, to appear, [arXiv:2008.12310](https://arxiv.org/abs/2008.12310).
- [3] D. Cox: Toric residues, *Ark. Mat.* **34** (1996) 73–96.
- [4] D. Cox, J. Little, and H. Schenck: *Toric Varieties*, Graduate Studies in Mathematics, vol. 124, American Mathematical Society, 2011.
- [5] C. Fevola and C. Görgen: The mathematical research-data repository MathRepo, *Computer-algebra Rundbrief* **70** (2022) 16–20.
- [6] E. Gawrilow and M. Joswig: **Polymake**: a framework for analyzing convex polytopes, *Polytopes – Combinatorics and Computation*, pages 43–73, Springer, 2000.
- [7] A. Gelman, J. Carlin, H. Stern, D. Dunson, A. Vehtari, D. Rubin: *Bayesian Data Analysis*, Third edition, Texts in Statistical Science Series, Chapman & Hall, Boca Raton, FL, 2014.
- [8] S. Hossten, A. Khetan, and B. Sturmfels: Solving the likelihood equations, *Found. Comput. Math.* **5** (2005) 389–407.
- [9] M. Kaluba, B. Lorenz, and S. Timme: **Polymake.jl**: A new interface to polymake, *International Congress on Mathematical Software*, pages 377–385. Springer, 2020.
- [10] S. Lin, B. Sturmfels, and Z. Xu: *Marginal likelihood integrals for mixtures of independence models*, *Journal of Machine Learning Research* **10** (2009) 1611–1631.
- [11] D. Maclagan and B. Sturmfels: *Introduction to Tropical Geometry*, Graduate Studies in Mathematics, vol. 161, American Mathematical Soc., 2009.

- [12] L. Nilsson and M. Passare: Mellin transforms of multivariate rational functions, *J. Geom. Anal.* **23** (2013) 24–46.
- [13] D. Stirzaker: *Elementary Probability*, 2nd edition, Cambridge University Press, 2003.
- [14] B. Sturmfels and S. Telen: Likelihood equations and scattering amplitudes, *Algebraic Statistics* **12** (2021) 167–186.
- [15] S. Sullivant: *Algebraic Statistics*, Graduate Studies in Mathematics, 194, American Mathematical Society, Providence, RI, 2018.
- [16] S. Telen: Numerical root finding via Cox rings, *J. Pure Appl. Algebra* **224** (2020), no. 9.
- [17] S. Telen: Introduction to Toric Geometry, [arXiv:2203.01690](https://arxiv.org/abs/2203.01690).
- [18] A. J. Walker: New fast method for generating discrete random numbers with arbitrary frequency distributions, *Electronics Letters* **10** (1974) 127–128.

Authors' addresses:

Michael Borinsky, Institute for Theoretical Studies, ETH Zürich	michael.borinsky@eth-its.ethz.ch
Anna-Laura Sattelberger, MPI-MiS Leipzig	anna-laura.sattelberger@mis.mpg.de
Bernd Sturmfels, MPI-MiS Leipzig and UC Berkeley	bernd@mis.mpg.de
Simon Telen, MPI-MiS Leipzig	simon.telen@mis.mpg.de